

Universal Adversarial Perturbations: Efficiency on a small image dataset

Waris Radji*

Index Terms—Computer vision, Image classification, Deep neural networks, Adversarial attack.

ABSTRACT

Although neural networks perform very well on the image classification task, they are still vulnerable to adversarial perturbations that can fool a neural network without visibly changing an input image. A paper has shown the existence of Universal Adversarial Perturbations which when added to any image will fool the neural network with a very high probability. In this paper we will try to reproduce the experience of the Universal Adversarial Perturbations paper, but on a smaller neural network architecture and training set, in order to be able to study the efficiency of the computed perturbation.

1 INTRODUCTION

As part of my engineering school's introductory research program, I aim to reproduce a scientific experiment. I chose to reproduce the **universal adversarial perturbations** paper experiments introduced by Seyed-Mohsen Moosavi-Dezfooli *et al* accepted at IEEE Conference on Computer Vision and Pattern Recognition (CVPR) in 2017[1].

In image classification, an adversarial perturbation is a vector that when added to an image cause the network output to change drastically with making quasi-imperceptible changes to the input image. Universal adversarial perturbations (UAPs) correspond to a single vector that will fool the neural network on any image with very high probability (see Fig.1). These perturbations have many applications in the real world, for example in CAPTCHA tests when a user has to associate an image with a label or in steganography to hide information in images[2]. They can also be used for hostile purposes, knowing that they are very difficult to detect with the naked eye.

The **reference paper** [1] has already demonstrated the existence and efficiency of UAPs, on large neural network architecture (CaffeNet, VGG-F, VGG-16, VGG-19, GoogLeNet, and ResNet-152) and with the very large image dataset of ImageNet Large Scale Visual Recognition Challenge 2012 (ILSVRC2012). In this paper we will try to reproduce some of their results, with VGG-11 [5] neural network architecture which is smaller than those studied in the paper and on the Visual Object Classes Challenge 2012 (VOC2012) [4] dataset which is 1,000 times smaller than ILSVRC2012:

*Student in the introductory research program of Bordeaux Institute of Technology - ENSEIRB-MATMECA School of Engineering.

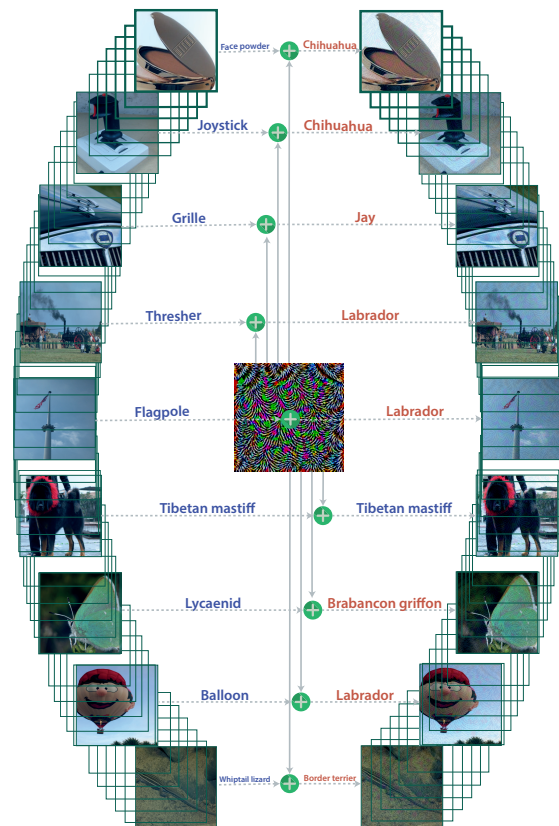


Fig. 1: This figure is taken from the reference article. When added to a natural image, a universal perturbation image causes the image to be misclassified by the deep neural network with high probability. Left images: Original natural images. The labels are shown on top of each arrow. Central image: Universal perturbation. Right images: Perturbed images.

- We will train a neural network;
- We will compute the UAP with parameters quasi-similar to the paper one;
- We will observe dominant labels founded by the algorithm;
- We will compare the computed UAP to other perturbations.

All the code that allowed me to achieve my experiments can be found on [Github](#).

2 UNIVERSAL ADVERSARIAL PERTURBATIONS COMPUTATION

Before conclusions can be drawn from the UAPs, the method by which they are estimated must be studied.

2.1 Notations and terminology

The important mathematical notations used in the reference paper will be explained in this section.

- μ : the distribution of images in \mathbb{R}^d .
- $x \sim \mu$: an non-perturbed input image.
- v : the universal perturbation vector (UAP).
- $X = \{x_1, \dots, x_n\}$: a set of images sampled from the distribution μ . Input of the algorithm 1.
- X_v : X for which each image is summed with v . The perturbed set.
- \hat{k} : a classification function that outputs for each image $x \in \mathbb{R}^d$ an estimated label $\hat{k}(x)$.
- Δv_i : minimal perturbation that sends the current perturbed point $x_i + v$ to the decision boundary of the classifier.
- *fooling rate*: the proportion of total perturbed images $(x + v)$ in a dataset for which $\hat{k}(x + v) \neq \hat{k}(x)$
- ξ : parameter of the algorithm 1 that controls the magnitude of v .
- δ : parameter algorithm 1 that quantifies the desired fooling rate for all images in X .

We seek a vector v such that

$$\hat{k}(x + v) \neq \hat{k}(x) \text{ for "most" } x \sim \mu$$

In simple words, the UAP that maximizing the fooling rate. There are two constraints to find v :

- 1) $\|v\|_p \leq \xi$,
- 2) $\mathbb{P}_{x \sim \mu} (\hat{k}(x + v) \neq \hat{k}(x)) \geq 1 - \delta$.

The first constraint ensures the quasi-imperceptible nature of the UAP, and the second allows the Algorithm 1 to iterate until the desired fooling rate is reached.

2.2 Algorithm

Until the desired fooling rate is not reached (it is also possible to define a maximum number of iterations) the algorithm takes each well classified data point in X and computes the minimal perturbation Δv_i that sends the current perturbed point $x_i + v$ to the decision boundary of the classifier as illustrated in Fig. 2. Δv_i is computed by solving the following optimisation problem :

$$\Delta v_i \leftarrow \arg \min_r \|r\|_2 \text{ s.t. } \hat{k}(x_i + v + r) \neq \hat{k}(x_i). \quad (1)$$

The resolution of Equation 1 is allowed by the *DeepFool* algorithm [6] of the same authors which computes the minimal perturbation of a single image. To control the norm of the vector v according to the parameter ξ , the updated perturbation vector is projected on the ℓ_p ball of radius ξ and centered at 0. The projection operator $\mathcal{P}_{p,\xi}$ is defined as follows:

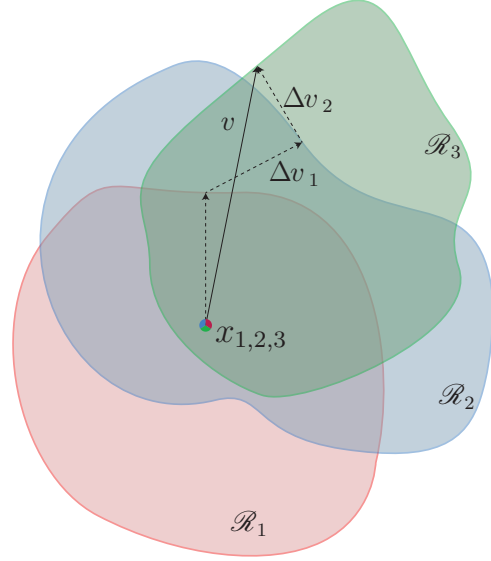


Fig. 2: This figure is taken from the reference article. Schematic representation of the algorithm used to compute universal perturbations. In this illustration, data points x_1, x_2 and x_3 are super-imposed, and the classification regions \mathcal{R}_i (i.e., regions of constant estimated label) are shown in different colors. Our algorithm proceeds by aggregating sequentially the minimal perturbations sending the current perturbed points $x_i + v$ outside of the corresponding classification region \mathcal{R}_i .

$$\mathcal{P}_{p,\xi}(v) = \arg \min_{v'} \|v - v'\|_2 \text{ subject to } \|v'\|_p \leq \xi.$$

The updated vector v is given by $v \leftarrow \mathcal{P}_{p,\xi}(v + \Delta v_i)$.

The detailed algorithm is provided in Algorithm 1. Based on the `code` provided by the authors, I was able to adapt this algorithm to *Pytorch* for my experiment.

Algorithm 1 Computation of universal perturbations.

- 1: **input:** Data points X , classifier \hat{k} , desired ℓ_p norm of the perturbation ξ , desired accuracy on perturbed samples δ .
 - 2: **output:** Universal perturbation vector v .
 - 3: Initialize $v \leftarrow 0$.
 - 4: **while** $\text{Err}(X_v) \leq 1 - \delta$ **do**
 - 5: **for** each datapoint $x_i \in X$ **do**
 - 6: **if** $\hat{k}(x_i + v) = \hat{k}(x_i)$ **then**
 - 7: Compute the *minimal* perturbation that sends $x_i + v$ to the decision boundary:

$$\Delta v_i \leftarrow \arg \min_r \|r\|_2 \text{ s.t. } \hat{k}(x_i + v + r) \neq \hat{k}(x_i).$$
 - 8: Update the perturbation:

$$v \leftarrow \mathcal{P}_{p,\xi}(v + \Delta v_i).$$
 - 9: **end if**
 - 10: **end for**
 - 11: **end while**
-

TABLE 1: Comparison between VOC2012 and ILSVRC2012

Criterion	VOC2012	ILSVRC2012
Number of images	Both 5,000 images in training and validation set.	1.28 million training images, and 50 thousand validation image.
Number of classes	20	1000
Variety of classes	Both datasets contains a variety of objects and living things. ILSVRC2012 divides its data more than VOC2012, for example the cat class of VOC2012 is divided into cat breeds in ILSVRC2012 (Egyptian, Persian, tiger, Siamese, etc...).	
Image size	About 300×300	

Both dataset are similar with respect to the average number of object instances and the amount of clutter per image.

3 UNIVERSAL PERTURBATION OF VGG-11 NEURAL NETWORK ARCHITECTURE

In this section we will reproduce the experiment of the reference paper [1] which consists in computing an UAP, based on the VGG-11 neural network architecture [5] and on the VOC212 dataset [4].

3.1 The VOC2012 dataset

Not having the computational resources of the authors of the article, I chose to use the VOC2012 dataset which is quite similar to the ILSVRC2012 dataset which is used in the article, but much smaller. Table 1 presents a summary of the comparison of the two datasets. The twenty VOC2012 classes can be seen in detail in Table 2.

Person	Person
Animal	bird, cat, cow, dog, horse, sheep
Vehicle	aeroplane, bicycle, boat, bus, car, motorbike, train
Indoor	bottle, chair, dining table, potted plant, sofa, tv/monitor

TABLE 2: The twenty object classes of VOC2012

3.2 Training VGG-11 neural network

For the architecture of the neural network, I chose VGG-11 which is quite similar to some of the architectures studied in the reference paper (VGG-16, VGG-19), but which has fewer convolutional layers, thus fewer parameters. This architecture is have a higher classification error rate.

Instead of taking a randomly initialized VGG-11 model, *Torchvision* offers pre-trained models. The *Torchvision* models have been trained on the ImageNet dataset. In our case VOC2012 containing only 20 classes. To adapt the pre-trained model we define a new final layer which has an input size equal to the layer we are replacing (4096), but with an output of 20 classes. This new layer is randomly initialized and is the only part of our model that does not have pre-trained parameters.

To load the data into the model, simply follow the *Torchvision* instructions :

All pre-trained models expect input images normalized in the same way, i.e. mini-batches of 3-channel RGB images of shape $(3 \times H \times W)$, where H and W are expected to be at least 224. The images have to be loaded in to a range of $[0, 1]$ and then normalized using $\text{mean} = [0.485, 0.456, 0.406]$ and $\text{std} = [0.229, 0.224, 0.225]$.

We finally reach an accuracy score of 75% on the validation dataset. Considering that VOC2012 is also a dataset that is used for image segmentation, which means that an image can have several labels (e.g. a person walking his dog), which biases the model. For ease of use, the score is based on only one of the true labels of the image.

3.3 Computation of the UAP

Now that we have our classifier, we can compute the UAP, by using the algorithm 1 with the parameters $\xi = 2000$ for the norm ℓ_2 , and a desired fooling rate δ of 0.80. The implementation of the algorithm has been slightly modified to be adapted to *Pytorch* on GPU and to reduce memory usage.

The image set X was chosen by taking 50 images per class from the validation dataset, i.e. a total of 1000 images. Due to the small volume of data compared to the reference paper (10,000 images), it was not possible to reach the desired fooling rate of 80%, but a fooling rate of 56% was achieved, which is consistent with an experiment in the paper that showed that the fooling rate was strongly dependent on the size of X .

It is now possible to visualise the UAP that corresponds to the VGG-11 architecture in Figure 3. The perturbation obtained is very different from those obtained in the reference paper (see Figure 6).

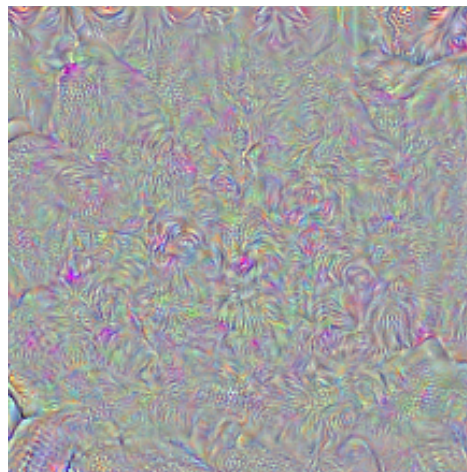


Fig. 3: UAP computed for VGG-11 architecture.

Figure 4 shows the results of adding the UAP on images from the VOC2012 validation set. The UAP is quasi-imperceptible but succeeds in fooling the neural network on a large number of images.



Fig. 4: Examples of perturbed images and their corresponding labels transformation.

4 DOMINANT LABELS

To better see the effect of UAP on natural images, we can view the label distribution of VOC2012. We build a directed graph $G = (V, E)$, whose vertices denote the labels, and weighted directed edges $e = (i \leftarrow j)$ indicate the number of label i are fooled into label j when applying the universal perturbation. The color of the vertex represents the category group (see Table 2) to which it belongs and the size of the node represents its indegree. The graph in Figure 5 was generated with the *Gephi* tool and the vertices were placed automatically with the *ForceAtlas2* [7] algorithm.

By observing the topology of the graph obtained, we can see that the *ForceAtlas2* algorithm has automatically (in an unsupervised way) grouped the labels belonging to the same category, which results in strong links between these labels. Labels belonging to the same category tend to have a relationship in terms of which label the neural network will be fooled into (e.g. cat and dog). It is possible to see some labels stand out by their sizes. These labels are called in the reference article the *dominant labels*, and the perturbations are mostly formed from these labels. The hypothesis in the reference article to explain this, is that these dominant labels occupy large regions in the image space, and therefore represent good candidate labels for fooling most natural images.

5 COMPARING WITH OTHER PERTURBATIONS

In this section we will try to understand the unique characteristics of universal perturbations by comparing our perturbations with other ones:

- A random perturbation;
- UAPs computed by the Algorithm 1 but for VGG-16 (Figure 6a) and VGG-19 (Figure 6b) neural network architecture and on ILSCVR 2012 data.

First, let's compare our UAP to a random vector. Figure 7 shows how the label evolves as a relation to the intensity of the perturbation on the image (perturbations are scaled up). Note that on average, a perturbation of ℓ_2 norm 2000 represents less than 5% of the pixels in the clean image.

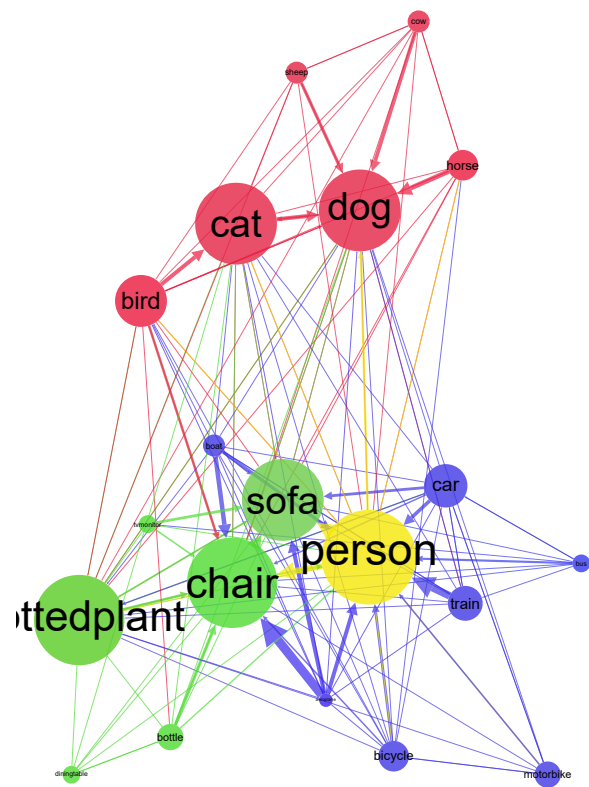


Fig. 5: Representation of the graph $G = (V, E)$, where the vertices are the set of labels, and weighted directed edges $i \rightarrow j$ indicate the number of label i are fooled into label j when applying the universal perturbation.

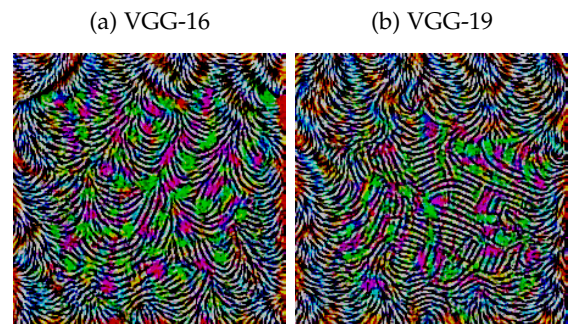


Fig. 6: UAPs from the reference paper

The UAP (Figure 7a) manages to fool the neural network on the cat image with a norm of 2,000 while the random vector (Figure 7b) must reach a norm of 8,000.

To generalize this observation we display a curve on the graph in Figure 8 that shows the fooling rate on the validation set of VOC2012 for each perturbation.

The fact that our UAP (black curve) is more efficient than a random vector seems to be confirmed: it needs a norm of 2000 for the UAP to fool 40% of the validation set, while it needs a norm of 10,000 for the random vector. The reference paper explains this by suggests that the UAPs exploits some geometric correlations between different parts of the decision boundary of the classifier.

We can also observe the generalization property of UAPs

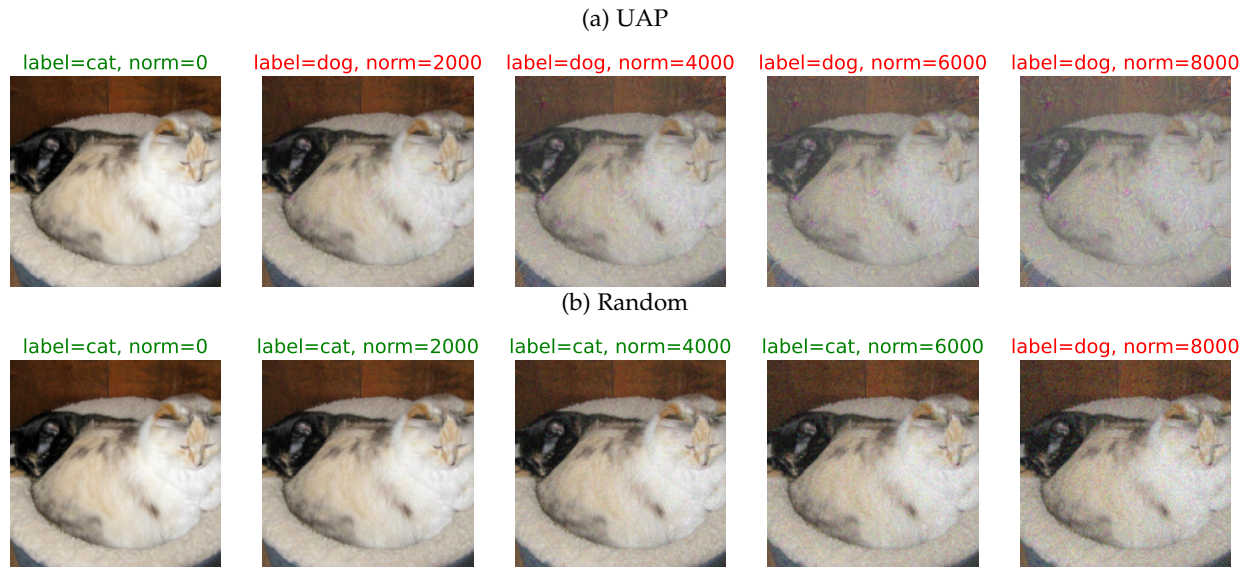


Fig. 7: Evolution of the neural network fooling by varying the perturbation norm

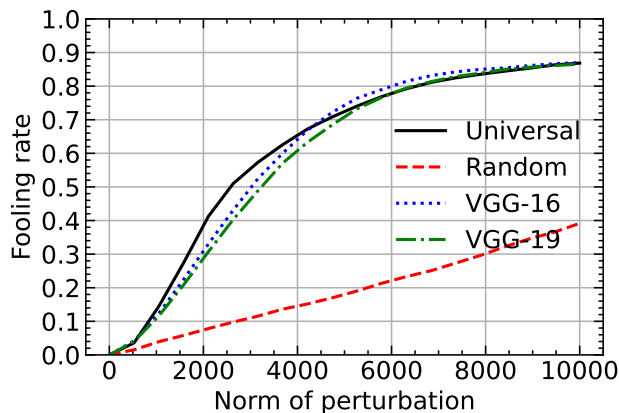


Fig. 8: Comparison between fooling rates of different perturbations.

across different neural network architectures. Although the UAPs of VGG-16 and VGG-19 were not trained on the same data and the UAPs are very different, they have very similar results to our UAP on the VOC2012 validation set. This may be a negligible difference, but at around the original norm of our UAP (2,000), our UAP seems to perform slightly better than the other two. I suggest that this is because for the 2,000 norm, our UAP is really very specialised in relation to the data it has learned from.

We can therefore imagine a modification of Algorithm 1, to specialise an existing UAP on another architecture, which would consist of taking a pre-calculated vector as input instead of the null vector, to speed up the start of the algorithm and to be able to slightly increase the fooling rate scores. A kind of Transfer Learning applied to UAPs.

6 CONCLUSIONS

After training a VGG11 neural network on the VOC2012 dataset, we were able to calculate an UAP from the resulting classifier. Despite the size of our dataset, we were able to

fool the classifier. We then noticed the existence of dominant labels that contributed much more to the formation of the UAP. Finally we compared our UAP with the random vector and UAPs calculated from other architecture. We saw that our UAP is really more efficient than the random vector, but that it has almost the same performance as the one computed from other neural network architectures (and a much larger dataset).

ACKNOWLEDGMENTS

I thank the authors of this paper, it was a pleasure to work on such an interesting subject;

I thank Dr. Michael Clément (Associate professor at Bordeaux Institute of Technology - ENSEIRB-MATMECA School of Engineering) who was a very good supervisor for this work;

I thank my friend Hector Piteau for giving me the possibility to access good computational resources for my experiments.

REFERENCES

- [1] Seyed-Mohsen Moosavi-Dezfooli, Alhussein Fawzi, Omar Fawzi and Pascal Frossard. Universal adversarial perturbations, 2016; [arXiv:1610.08401](https://arxiv.org/abs/1610.08401).
- [2] Salah Ud Din and Naveed Akhtar and Shahzad Younis and Faisal Shafait and Atif Mansoor and Muhammad Shafique Steganographic universal adversarial perturbations, Pattern Recognition Letters Volume 135.
- [3] Olga Russakovsky and Jia Deng and Hao Su and Jonathan Krause and Sanjeev Satheesh and Sean Ma and Zhiheng Huang and Andrej Karpathy and Aditya Khosla and Michael Bernstein and Alexander C. Berg and Li Fei-Fei ImageNet Large Scale Visual Recognition Challenge, International Journal of Computer Vision, 2015.
- [4] Everingham, M. and Van Gool, L. and Williams, C. K. I. and Winn, J. and Zisserman, A. The PASCAL Visual Object Classes Challenge 2012 (VOC2012) Results
- [5] Karen Simonyan and Andrew Zisserman. Very Deep Convolutional Networks for Large-Scale Image Recognition, 2014; [arXiv:1409.1556](https://arxiv.org/abs/1409.1556).
- [6] Seyed-Mohsen Moosavi-Dezfooli, Alhussein Fawzi and Pascal Frossard. DeepFool: a simple and accurate method to fool deep neural networks, 2015; [arXiv:1511.04599](https://arxiv.org/abs/1511.04599).
- [7] Jacomy M, Venturini T, Heymann S, Bastian M. ForceAtlas2, a continuous graph layout algorithm for handy network visualization designed for the Gephi software.